## 2.1 Introduction

To describe the mechanism of steady current drive in our experiments we follow the simplest physical MHD model of non-linear Hall-effect current drive developed by HUGRASS and JONES and given in the paper of JONES(1984). In this model the ions are assumed immobile and uniformly distributed and the electrons are treated as an inertialess, pressureless, negatively charged fluid.

The large-aspect-ratio limit is taken, in which we consider an infinitely long plasma cylinder of radius $a$. Appropriately phased radio-frequency currents are passed through a series of helical coils of pitch length $\ell$ which are wound around the plasma at a radius $a$. We define a wavenumber associated with the coil structure, $k = 2\pi/\ell$. The antenna is shown schematically in Figure 2.1a.

The analysis presented in this chapter is based on the mathematical techniques used in the paper by DUTCH,MCCARTHY AND STORER(1986). This paper will be referred to later as simply DMS(1986). As pointed out by BERTRAM(Private Communication, 1986), this paper made the incorrect assumption that that the radial component of the oscillating plasma screening current must vanish at the axis ($r = 0$). The current drive analysis in this chapter is an independent calculation using the original techniques, for which the basic equations and their numerical solutions have been independently revised and used with the correct boundary conditions.

The solutions which BERTRAM(1987) obtained when he reworked the DMS(1986) publication showed some minor differences when compared with the analysis presented in this chapter. Numerical solutions obtained using the two codes written to solve the basic equations have been compared for four distinct combinations of chosen plasma parameters and external fields. In all four cases reasonable agreement was shown between corresponding numerical solutions, thus giving confidence in each code. The most recently published results of BERTRAM(1988) are very closely reproduced with the numerical code written by the present author.

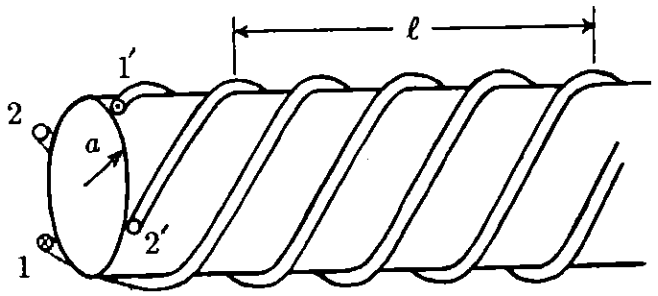


(a)

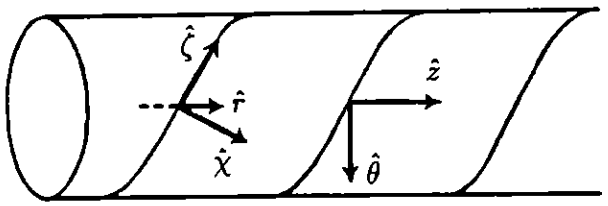


(b)

FIGURE 2.1(a) Schematic diagram showing the $m = 1$ double-helix coil structure used to drive steady toroidal and poloidal current. The coils are shown in the large aspect ratio limit for clarity. 2.1(b) The helical $(\hat{r}, \hat{\chi}, \hat{\zeta})$ and cylindrical $(\hat{r}, \hat{\theta}, \hat{z})$ cooordinate systems used in the analysis.

## 2.2 The Helical Coordinate System

In this section we introduce a helical coordinate system naturally related to the coil structure and shown schematically in Figure 2.1b. The particular choice of coordinate system and the vector algebra which follows is largely based on the work of RYU(1983). Use of this helical coordinate system leads to considerable simplification of the equations governing the plasma. However, as pointed out by RYU(1983), there appear to be inherent difficulties associated with the use of helical coordinates, which puts them in a different class to those curvilinear coordinate systems found treated in textbooks.

A general poloidal (azimuthal) mode number $m$ is retained in the analysis, although for the present experiments with double helical coils, $m = 1$.

Consider a helical coordinate system based on the unit vectors $\hat{r}, \hat{\chi}$ and $\hat{\zeta}$ where $\hat{r}$ is the usual radial unit vector in cylindrical coordinates $(\hat{r}, \hat{\theta}, \hat{z})$ and :

$$\begin{aligned} & & \hat{\chi} &= \frac{\nabla\chi}{|\nabla\chi|} \quad \text{with} \quad \chi = m\theta + kz \\ \text{and} & & \hat{\zeta} &= \hat{r} \times \hat{\chi} \\ \text{Then} & & \hat{\chi} &= \frac{m\hat{\theta} + kr\hat{z}}{k_0 r} \\ & & \hat{\zeta} &= \frac{-kr\hat{\theta} + m\hat{z}}{k_0 r} \\ \text{where} & & k_0 &= (k^2 + \frac{m^2}{r^2})^{\frac{1}{2}} \end{aligned} \tag{2.1}$$

The $\hat{\zeta}$ coordinate axis is chosen to be along the direction defined by the external helical driving coils, so that in the large aspect ratio limit considered here we have $\partial/\partial\zeta \equiv 0$. In the limit $k = 0$ where the windings are straight and parallel, $\hat{\chi}$ corresponds to $\hat{\theta}$ and $\hat{\zeta}$ corresponds to $\hat{z}$.

We can express an arbitrary vector $\boldsymbol{A}$ as :

$$\begin{aligned} \boldsymbol{A} &= A_r\hat{r} + A_\theta\hat{\theta} + A_z\hat{z} \\ &= A_r\hat{r} + A_\chi\hat{\chi} + A_\zeta\hat{\zeta} \end{aligned}$$

so that

$$A_\chi = \frac{mA_\theta + krA_z}{k_0 r} \tag{2.2}$$

$$A_\zeta = \frac{-krA_\theta + mA_z}{k_0 r} \tag{2.3}$$

or

$$A_\theta = \frac{mA_\chi - krA_\zeta}{k_0 r} \tag{2.4}$$

$$A_z = \frac{krA_\chi + mA_\zeta}{k_0 r} \tag{2.5}$$

In order to express Maxwell's equations and the generalised Ohm's law in helical coordinates it is necessary to determine the appropriate form of the differential operators. The correct form of the required operators can be obtained from their form in cylindrical coordinates, using the coordinate transformation equations (2.2)→(2.5).

If the components of $\boldsymbol{A}$ or the scalar $\psi$ vary as $\exp(im\theta + ikz) = \exp i\chi$ , then using the definition of $k_0$ given in equation (2.1) we obtain :

$$\nabla\psi = \hat{r}\frac{\partial\psi}{\partial r} + \hat{\chi}\, ik_0\psi \tag{2.6}$$

$$\nabla\cdot\boldsymbol{A} = \frac{1}{r}\frac{\partial}{\partial r}(rA_r) + ik_0A_\chi \tag{2.7}$$

$$\begin{aligned}\nabla\times\boldsymbol{A} &= \hat{r}\,[ik_0A_\zeta\,] \\ &+ \hat{\chi}\left[\frac{-1}{k_0r}\frac{\partial}{\partial r}(k_0rA_\zeta)\right] \\ &+ \hat{\zeta}\left[-ik_0A_r + k_0\frac{\partial}{\partial r}\left(\frac{A_\chi}{k_0}\right) - \frac{2mk}{k_0^2r^2}A_\zeta\right]\end{aligned} \tag{2.8}$$

$$\begin{aligned}(\nabla\times\nabla\times\boldsymbol{A})_r &= ik_0\left[-ik_0A_r + k_0\frac{\partial}{\partial r}\left(\frac{A_\chi}{k_0}\right) - \frac{2mk}{k_0^2r^2}A_\zeta\right] \\ (\nabla\times\nabla\times\boldsymbol{A})_\chi &= \frac{-1}{k_0r}\frac{\partial}{\partial r}\left\{k_0r\left[-ik_0A_r + k_0\frac{\partial}{\partial r}\left(\frac{A_\chi}{k_0}\right) - \frac{2mk}{k_0^2r^2}A_\zeta\right]\right\} \\ (\nabla\times\nabla\times\boldsymbol{A})_\zeta &= k_0^2A_\zeta - k_0\frac{\partial}{\partial r}\left\{\frac{1}{k_0^2r}\frac{\partial}{\partial r}(k_0rA_\zeta)\right\} \\ &- \frac{2mk}{k_0^2r^2}\left[-ik_0A_r + k_0\frac{\partial}{\partial r}\left(\frac{A_\chi}{k_0}\right) - \frac{2mk}{k_0^2r^2}A_\zeta\right]\end{aligned} \tag{2.9}$$

If the components of $\boldsymbol{A}$ are functions of $r$ only, then :

$$\nabla \times \boldsymbol{A} = \hat{\theta}\left[-\frac{\partial A_z}{\partial r}\right] + \hat{z}\left[\frac{1}{r}\frac{\partial}{\partial r}(rA_\theta)\right] \tag{2.10}$$

So, using equations (2.2)→(2.5) which relate the $\chi$ and $\zeta$ components of a vector to its $\theta$ and $z$ components and vice versa, we obtain :

$$\nabla \times \boldsymbol{A} = \hat{\chi}\left[\frac{-1}{k_0 r}\frac{\partial}{\partial r}(k_0 r A_\zeta)\right] + \hat{\zeta}\left[k_0\frac{\partial}{\partial r}\left(\frac{A_\chi}{k_0}\right) - \frac{2mk}{k_0^2 r^2}A_\zeta\right] \tag{2.11}$$

## 2.3 The Vacuum Fields

The externally applied currents can be approximated by the continuous distribution

$$\begin{aligned} \boldsymbol{j}_e &= \hat{\zeta}\frac{2I_e}{\pi a}\mathrm{Re}\{e^{i(\omega t + m\theta + kz)}\}\delta(r-a) \\ &= \hat{\zeta}\frac{2I_e}{\pi a}\cos(\omega t + \chi)\delta(r-a) \end{aligned} \tag{2.12}$$

where $I_e$ is the amplitude of the discrete RF currents in the helical coils. This particular current distribution produces a vacuum magnetic field (at $r = 0$) of the same amplitude as that made by the current $I_e$ flowing in discrete coils located at $r = a$. To achieve the same vacuum field strength, the total continuously distributed current must be larger than the corresponding discrete current by a factor of $4/\pi$.

The vacuum magnetic field produced by the current in the external coils is found from Maxwell's equations :

$$\nabla \times \boldsymbol{b}_e = \mu_0 \boldsymbol{j}_e \tag{2.13}$$

$$\nabla \times \boldsymbol{e}_e = -\frac{\partial \boldsymbol{b}_e}{\partial t} \tag{2.14}$$

Since these equations are linear both $\boldsymbol{b}_e$ and $\boldsymbol{e}_e$ vary as $e^{i(\omega t+\chi)}$ and combining equations (2.13) and (2.14) we have :

$$\nabla \times \nabla \times \boldsymbol{e}_e = -i\omega\mu_0 \boldsymbol{j}_e \tag{2.15}$$

With $\boldsymbol{j}_e$ as in equation (2.12) and using equation (2.9), $\boldsymbol{e}_e$ is given by :

$$-k_0\frac{\partial}{\partial r}\left\{\frac{1}{k_0^2 r}\frac{\partial}{\partial r}(k_0 r e_{e\zeta})\right\}+k_0^2 e_{e\zeta}=\frac{-2i\omega\mu_0 I_e}{\pi a}e^{i(\omega t+\chi)}\delta(r-a) \tag{2.16}$$

with the other components being obtained from :

$$-ik_0 e_{er}+k_0\frac{\partial}{\partial r}\left(\frac{e_{e\chi}}{k_0}\right)-\frac{2mk}{k_0^2 r^2}e_{e\zeta} = 0 \tag{2.17}$$

and

$$\frac{1}{r}\frac{\partial}{\partial r}(r e_{er})+ik_0 e_{e\chi} = 0 \tag{2.18}$$

the latter equation being $\nabla\cdot\boldsymbol{e}_e=0$.

The solution to equation (2.16) is :

$$\begin{aligned} e_{e\zeta} &= \frac{-2i\omega\mu_0 I_e}{\pi a}\frac{a}{k_0(a)}\frac{k^2 r I_m'(kr)K_m'(ka)}{k_0 r}e^{i(\omega t+\chi)} \qquad r<a \\ &= \frac{-2i\omega\mu_0 I_e}{\pi a}\frac{a}{k_0(a)}\frac{k^2 r K_m'(kr)I_m'(ka)}{k_0 r}e^{i(\omega t+\chi)} \qquad r>a \end{aligned} \tag{2.19}$$

where $k_0(a)=k_0(r=a)$ and the constants of proportionality have been chosen to give the correct jump in the derivative at $r=a$. $I_m$ and $K_m$ are modified Bessel functions of the first and second kind respectively. The prime denotes differentiation with respect to the argument $kr$.

Using equations (2.14) and (2.8) we can obtain $\boldsymbol{b}_e$ from the solution for $e_{e\zeta}$ given in equation (2.19). For $r<a$ and the case $m=1$ we find :

$$b_{er} = -2iB_\omega I_1'(kr)e^{i(\omega t+\chi)} \tag{2.20}$$

$$b_{e\chi} = 2B_\omega\frac{k_0 I_1(kr)}{k}e^{i(\omega t+\chi)} \tag{2.21}$$

$$b_{e\zeta} = 0 \tag{2.22}$$

where

$$B_\omega = -\frac{\mu_0 I_e}{\pi a}\frac{k^2 a}{k_0(a)}K_1'(ka) \tag{2.23}$$

Adding the complex conjugate to the field components above, we obtain the total field produced by the external current distribution $\boldsymbol{j}_e$ :

$$\boldsymbol{b}_e=2B_\omega\left[I_1'(kr)\sin(\omega t+\chi)\hat{r}+\frac{k_0 I_1(kr)}{k}\cos(\omega t+\chi)\hat{\chi}\right] \tag{2.24}$$

In the limit $k = 0$ where the RF conductors are straight and parallel, this magnetic field corresponds to a transverse rotating magnetic field of amplitude $B_\omega$ and frequency $\omega$. Figure 2.2 is a plot of the on-axis field amplitude $B_\omega$ [normalised to $B_\omega(ka = 0)$], against $ka$ for fixed external RF coil current $I_e$. The decrease in $B_\omega$ with increasing $ka$ (for a given plasma of fixed radius $a$) is a geometrical effect due to the decreasing pitch length of the helical windings.

## 2.4 Basic Equations

The total fields and currents in the plasma will be obtained from a self-consistent solution of Maxwell's equations and Ohm's law. Thus we require :

$$\nabla \times \boldsymbol{E} = -\frac{\partial \boldsymbol{B}}{\partial t} \tag{2.25}$$

$$\nabla \times \boldsymbol{B} = \mu_0 \boldsymbol{J} \tag{2.26}$$

along with Ohm's law including the Hall term :

$$\boldsymbol{E} = \eta \boldsymbol{J} + \frac{1}{ne} \boldsymbol{J} \times \boldsymbol{B} \tag{2.27}$$

In general the currents in the external coils will produce fields which can be expressed as a full Fourier series in both $\chi$ and $\zeta$. However, HUGRASS(1985) has shown that for $m = 1$ and $k = 0$ the general solution (at long times, when the transient effects are not important) is given quite accurately by just the zero and first order harmonic terms. Thus we extend this to the present analysis and make the approximations :

$$\boldsymbol{B} = \boldsymbol{B}_0(r) + \frac{1}{2}\boldsymbol{b}(r,\chi,t) + \frac{1}{2}\boldsymbol{b}^*(r,\chi,t) \tag{2.28}$$

$$\boldsymbol{E} = \boldsymbol{E}_0(r) + \frac{1}{2}\boldsymbol{e}(r,\chi,t) + \frac{1}{2}\boldsymbol{e}^*(r,\chi,t) \tag{2.29}$$

$$\boldsymbol{J} = \boldsymbol{J}_0(r) + \frac{1}{2}\boldsymbol{j}(r,\chi,t) + \frac{1}{2}\boldsymbol{j}^*(r,\chi,t) \tag{2.30}$$

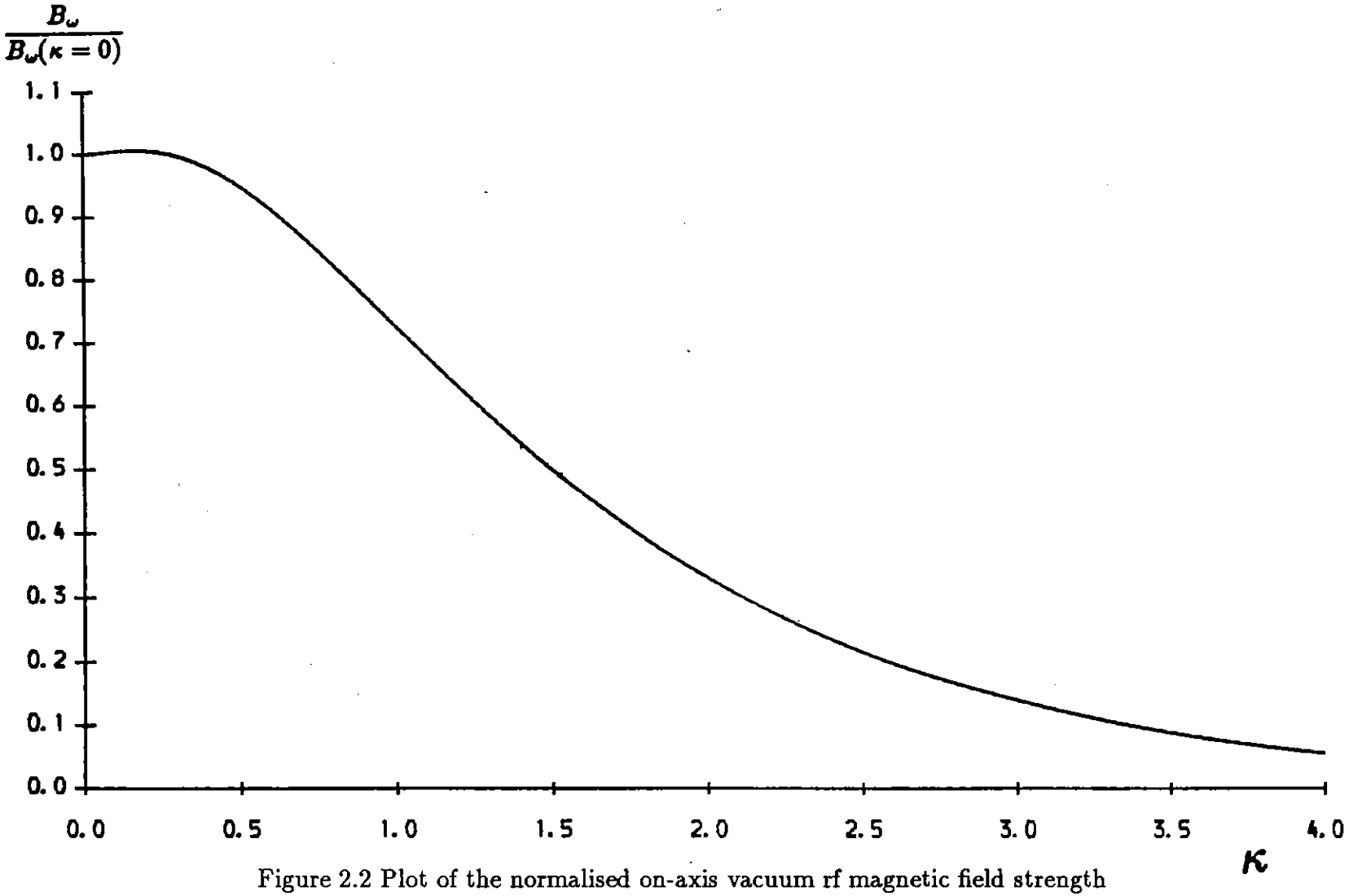


Figure 2.2 Plot of the normalised on-axis vacuum rf magnetic field strength $B_\omega/B_\omega(\kappa=0)$ versus $\kappa = ka$, for fixed rf coil current $I_e$. The values of $B_\omega$ are calculated from equation (2.23) and are normalised to $B_\omega(\kappa=0) = \mu_0 I_e/\pi a$.

where $\boldsymbol{b}, \boldsymbol{e}$ and $\boldsymbol{j}$ are all proportional to $e^{i(\omega t+\chi)}$. The asterisk denotes the complex conjugate. Substituting the above expressions into equations (2.25)→(2.27) and neglecting higher harmonics than the first, we obtain :

$$\nabla \times \boldsymbol{E}_0 = 0 \tag{2.31}$$

$$\nabla \times \boldsymbol{e} = -i\omega \boldsymbol{b} \tag{2.32}$$

$$\nabla \times \boldsymbol{B}_0 = \mu_0 \boldsymbol{J}_0 \tag{2.33}$$

$$\nabla \times \boldsymbol{b} = \mu_0 \boldsymbol{j} \tag{2.34}$$

$$\boldsymbol{E}_0 = \eta \boldsymbol{J}_0 + \frac{1}{ne}\left(\boldsymbol{J}_0 \times \boldsymbol{B}_0 + \frac{1}{4}\boldsymbol{j} \times \boldsymbol{b}^* + \frac{1}{4}\boldsymbol{j}^* \times \boldsymbol{b}\right) \tag{2.35}$$

$$\boldsymbol{e} = \eta \boldsymbol{j} + \frac{1}{ne}(\boldsymbol{j} \times \boldsymbol{B}_0 + \boldsymbol{J}_0 \times \boldsymbol{b}) \tag{2.36}$$

For the left-hand sides of equations (2.31)→(2.34) we use the explicit forms of the curl operator given in equations (2.8),(2.10) and (2.11).

Since $\boldsymbol{E}_0$ is a function of $r$ only, equation (2.31) expressed in cylindrical coordinates is :

$$\frac{\partial E_{0z}}{\partial r}\hat{\theta} - \frac{1}{r}\frac{\partial}{\partial r}(rE_{0\theta})\,\hat{z} = 0 \tag{2.37}$$

If there are no externally imposed steady electric fields we can take $E_{0\theta} = E_{0z} = 0$ and hence $E_{0\chi} = E_{0\zeta} = 0$.

The $r$ component of equation (2.32) gives :

$$e_\zeta = -\frac{\omega}{k_0} b_r \tag{2.38}$$

which is used to eliminate $e_\zeta$ in favour of $b_r$ everywhere. After elimination of $e_\zeta$ using equation (2.38), the $\chi$ and $\zeta$ components of equation (2.32) yield :

$$\frac{\partial}{\partial r}(rb_r) = -ik_0 r b_\chi \tag{2.39}$$

$$k_0 \frac{\partial}{\partial r}\left(\frac{e_\chi}{k_0}\right) = ik_0 e_r - i\omega b_\zeta - \frac{2mk\omega}{k_0^3 r^2} b_r \tag{2.40}$$

Ampere's law for the steady field $\boldsymbol{B}_0$, equation (2.33), can be written :

$$k_0 \frac{\partial}{\partial r}\left(\frac{B_{0\chi}}{k_0}\right) = \mu_0 J_{0\zeta} + \frac{2mk}{k_0^2 r^2} B_{0\zeta} \tag{2.41}$$

$$\frac{\partial}{\partial r}(k_0 r B_{0\zeta}) = -k_0 r \mu_0 J_{0\chi} \tag{2.42}$$

The $r$ component of Ampere's law for the oscillatory field $\boldsymbol{b}$, equation (2.34), gives the algebraic equation :

$$\mu_0 j_r = ik_0 b_\zeta \tag{2.43}$$

which is used to eliminate $j_r$ everywhere in favour of $b_\zeta$. The $\zeta$ and $\chi$ components of equation (2.34) yield :

$$k_0 \frac{\partial}{\partial r}\left(\frac{b_\chi}{k_0}\right) = \mu_0 j_\zeta + ik_0 b_r + \frac{2mk}{k_0^2 r^2} b_\zeta \tag{2.44}$$

$$\frac{\partial}{\partial r}(k_0 r b_\zeta) = -k_0 r \mu_0 j_\chi \tag{2.45}$$

$\nabla \cdot \boldsymbol{B}_0 = 0$ and $\nabla \cdot \boldsymbol{J}_0 = 0$ imply $B_{0r} = 0$ and $J_{0r} = 0$ respectively, so that the steady component of Ohm's law, equation (2.35), when multiplied through by $\mu_0$ gives :

$$\begin{aligned} \eta \mu_0 J_{0\chi} &= -\frac{1}{2ne}\mathrm{Re}\{\mu_0 j_\zeta b_r^* - \mu_0 j_r b_\zeta^*\} \\ &= -\frac{1}{2ne}\mathrm{Re}\{\mu_0 j_\zeta b_r^*\} \end{aligned} \tag{2.46}$$

and

$$\begin{aligned} \eta \mu_0 J_{0\zeta} &= -\frac{1}{2ne}\mathrm{Re}\{\mu_0 j_r b_\chi^* - \mu_0 j_\chi b_r^*\} \\ &= -\frac{1}{2ne}\mathrm{Re}\{ik_0 b_\zeta b_\chi^* - \mu_0 j_\chi b_r^*\} \end{aligned} \tag{2.47}$$

where equation (2.43) has been used to eliminate $j_r$. The $r$ component of equation (2.35) yields an expression for the steady radial electric field $E_{0r}$. In the oscillatory component of Ohm's law, equation (2.36), we substitute for $j_r$ and $e_\zeta$ using equations (2.43) and (2.38) respectively. We obtain :

$$e_r = \frac{1}{ne}(j_\chi B_{0\zeta} - j_\zeta B_{0\chi} + J_{0\chi} b_\zeta - J_{0\zeta} b_\chi) + \frac{i\eta k_0}{\mu_0} b_\zeta \tag{2.48}$$

$$\eta j_\chi = e_\chi - \frac{1}{\mu_0 ne}(-ik_0 b_\zeta B_{0\zeta} + \mu_0 J_{0\zeta} b_r) \tag{2.49}$$

$$\eta j_\zeta = -\frac{\omega}{k_0} b_r - \frac{1}{\mu_0 ne}(ik_0 b_\zeta B_{0\chi} - \mu_0 J_{0\chi} b_r) \tag{2.50}$$

Equations (2.48)→(2.50) are algebraic expressions which are used to eliminate $e_r$, $j_\chi$ and $j_\zeta$ respectively. Elimination of $j_\zeta$ from equation (2.46) using equation (2.50) gives

$$\mu_0 J_{0\chi} = \frac{1}{k_0}\left[\frac{\mu_0 ne\omega |b_r|^2 - k_0^2 B_{0\chi}\mathrm{Im}\{b_\zeta b_r^*\}}{|b_r|^2 + 2n^2 e^2 \eta^2}\right] \tag{2.51}$$

Similarly, elimination of $j_\chi$ from equation (2.47) using equation (2.49) gives :

$$\mu_0 J_{0\zeta} = \left[ \frac{k_0 ne\eta \mathrm{Im}\{b_\zeta b_\chi^*\} + \mu_0 ne \mathrm{Re}\{e_\chi b_r^*\} - k_0 B_{0\zeta} \mathrm{Im}\{b_\zeta b_r^*\}}{|b_r|^2 + 2n^2 e^2 \eta^2} \right] \tag{2.52}$$

We can now express $j_\chi$ and $j_\zeta$ in terms of the variables $e_\chi, b_r, b_\chi, b_\zeta, B_{0\chi}$ and $B_{0\zeta}$ by substitution of $J_{0\chi}$ and $J_{0\zeta}$ from equations (2.51) and (2.52) into equations (2.49) and (2.50). Equations (2.39)→(2.42),(2.44) and (2.45) then constitute a closed set of four complex and two real first order coupled differential equations in the variables $e_\chi, b_r, b_\chi, b_\zeta, B_{0\chi}$ and $B_{0\zeta}$.

The set of differential equations are easier to solve if the fields and currents are suitably normalised. We thus introduce the normalised variables :

$$\begin{aligned} \mathbf{b} &= \frac{\boldsymbol{b}}{b_r(0)} \\ \mathbf{e} &= \frac{\boldsymbol{e}}{\omega a b_r(0)} \\ \mathbf{j} &= \frac{\boldsymbol{j}}{ne\omega a} \\ \mathbf{B_0} &= \frac{\boldsymbol{B_0}}{\mu_0 ne\omega a^2} \\ \mathbf{J_0} &= \frac{\boldsymbol{J_0}}{ne\omega a} \end{aligned}$$

and the normalised radial coordinate :

$$\mathrm{x} = \frac{r}{a} \tag{2.53}$$

where $b_r(0)$ is the amplitude of the radial component of the RF field at $\mathrm{x} = 0$ in the presence of plasma. We also define the useful dimensionless quantities :

$$\begin{aligned} \kappa &= ka \\ \kappa_0 &= k_0 a = \left( \kappa^2 + \frac{m^2}{\mathrm{x}^2} \right)^{\frac{1}{2}} \\ \lambda^2 &= \frac{a^2}{\delta^2} = \frac{\mu_0 \omega}{2\eta} a^2 \\ \gamma_\omega &= \frac{\omega_{ce}}{\nu_{ei}} = \frac{B_\omega}{ne\eta} \\ \gamma &= \frac{b_r(0)}{ne\eta} \end{aligned}$$

The parameter $\lambda$ is the ratio of the plasma radius $a$, to the classical skin depth $\delta$. The parameter $\gamma_\omega$ is the ratio of $\omega_{ce}$, the electron cyclotron frequency in the RF field $B_\omega$, to the electron-ion momentum transfer collision frequency $\nu_{ei}$. In the above definitions, $\eta = m_e\nu_{ei}/n_e e^2$, is the scalar resistivity. The quantity $2\lambda^2/\gamma = \mu_0 ne\omega a^2/b_r(0)$ can be used to renormalise the steady magnetic field to the strength of the RF magnetic field at x = 0. i.e.

$$\frac{\boldsymbol{B}_0}{b_r(0)} = \frac{2\lambda^2}{\gamma}\frac{\boldsymbol{B}_0}{\mu_0 ne\omega a^2}$$

The normalised form of equations (2.39)→(2.42) and (2.44)→(2.50) are :

$$\frac{\partial}{\partial \mathrm{x}}\left(\frac{\mathrm{e}_\chi}{\kappa_0}\right) = i\mathrm{e}_r - \frac{i}{\kappa_0^2\mathrm{x}}(\kappa_0 \mathrm{x} \mathrm{b}_\zeta) - \frac{2m\kappa}{\kappa_0^4\mathrm{x}^3}(\mathrm{x}\mathrm{b}_r) \tag{2.54}$$

$$\frac{\partial}{\partial \mathrm{x}}(\mathrm{x}\mathrm{b}_r) = -i\kappa_0^2\mathrm{x}\left(\frac{\mathrm{b}_\chi}{\kappa_0}\right) \tag{2.55}$$

$$\frac{\partial}{\partial \mathrm{x}}\left(\frac{\mathrm{b}_\chi}{\kappa_0}\right) = \frac{1}{\kappa_0}\frac{2\lambda^2}{\gamma}\mathrm{j}_\zeta + \frac{i}{\mathrm{x}}(\mathrm{x}\mathrm{b}_r) + \frac{2m\kappa}{\kappa_0^4\mathrm{x}^3}(\kappa_0 \mathrm{x} \mathrm{b}_\zeta) \tag{2.56}$$

$$\frac{\partial}{\partial \mathrm{x}}(\kappa_0 \mathrm{x} \mathrm{b}_\zeta) = -\frac{2\lambda^2}{\gamma}\kappa_0 \mathrm{x} \mathrm{j}_\chi \tag{2.57}$$

$$\frac{\partial}{\partial \mathrm{x}}\left(\frac{\mathrm{B}_{0\chi}}{\kappa_0}\right) = \frac{1}{\kappa_0}\mathrm{J}_{0\zeta} + \frac{2m\kappa}{\kappa_0^4\mathrm{x}^3}(\kappa_0 \mathrm{x} \mathrm{B}_{0\zeta}) \tag{2.58}$$

$$\frac{\partial}{\partial \mathrm{x}}(\kappa_0 \mathrm{x} \mathrm{B}_{0\zeta}) = -\kappa_0 \mathrm{x} \mathrm{J}_{0\chi} \tag{2.59}$$

with

$$\mathrm{J}_{0\chi} = \frac{1}{(|\mathrm{x}\mathrm{b}_r|^2 + \frac{2\mathrm{X}^2}{\gamma^2})}\left[\frac{1}{\kappa_0}|\mathrm{x}\mathrm{b}_r|^2 - \kappa_0\left(\frac{\mathrm{B}_{0\chi}}{\kappa_0}\right)\mathrm{Im}\{(\kappa_0 \mathrm{x} \mathrm{b}_\zeta)\mathrm{x}\mathrm{b}_r^*\}\right] \tag{2.60}$$

$$\mathrm{J}_{0\zeta} = \frac{1}{(|\mathrm{x}\mathrm{b}_r|^2 + \frac{2\mathrm{X}^2}{\gamma^2})}\left[\frac{\kappa_0 \mathrm{x}}{2\lambda^2}\mathrm{Im}\left\{(\kappa_0 \mathrm{x} \mathrm{b}_\zeta)\frac{\mathrm{b}_\chi^*}{\kappa_0}\right\} + \kappa_0 \mathrm{x}\ \mathrm{Re}\left\{\left(\frac{\mathrm{e}_\chi}{\kappa_0}\right)\mathrm{x}\mathrm{b}_r^*\right\} - \frac{1}{\kappa_0 \mathrm{x}}(\kappa_0 \mathrm{x} \mathrm{B}_{0\zeta})\mathrm{Im}\{(\kappa_0 \mathrm{x} \mathrm{b}_\zeta)\mathrm{x}\mathrm{b}_r^*\}\right] \tag{2.61}$$

and

$$\mathrm{e}_r = \frac{2\lambda^2}{\gamma}\frac{1}{\kappa_0 \mathrm{x}}\mathrm{j}_\chi(\kappa_0 \mathrm{x} \mathrm{B}_{0\zeta}) - \frac{2\lambda^2}{\gamma}\kappa_0 \mathrm{j}_\zeta\left(\frac{\mathrm{B}_{0\chi}}{\kappa_0}\right) + \frac{1}{\kappa_0 \mathrm{x}}\mathrm{J}_{0\chi}(\kappa_0 \mathrm{x} \mathrm{b}_\zeta) - \kappa_0 \mathrm{J}_{0\zeta}\left(\frac{\mathrm{b}_\chi}{\kappa_0}\right) + \frac{i}{2\lambda^2}\frac{1}{\mathrm{x}}(\kappa_0 \mathrm{x} \mathrm{b}_\zeta) \tag{2.62}$$

$$j_\chi = \gamma\left[\kappa_0\left(\frac{e_\chi}{\kappa_0}\right) + \frac{i}{\kappa_0 x^2}(\kappa_0 x b_\zeta)(\kappa_0 x B_{0\zeta}) - \frac{1}{x}J_{0\zeta}(x b_r)\right] \quad (2.63)$$

$$j_\zeta = -\gamma\left[\frac{1}{\kappa_0 x}(x b_r) + \frac{i\kappa_0}{x}(\kappa_0 x b_\zeta)\left(\frac{B_{0\chi}}{\kappa_0}\right) - \frac{1}{x}J_{0\chi}(x b_r)\right] \quad (2.64)$$

## 2.5 Boundary Conditions

The boundary conditions given here are for the case $m = 1$ and are written in terms of the normalised variables introduced in the previous section.

From the requirement that the fields and currents must be continous at the axis ($x = 0$), we obtain the following conditions :

$$b_\zeta(0) = 0 \quad (2.65)$$

$$e_\zeta(0) = 0 \quad (2.66)$$

$$j_\zeta(0) = 0 \quad (2.67)$$

$$B_{0\chi}(0) = 0 \quad (2.68)$$

$$J_{0\chi}(0) = 0 \quad (2.69)$$

Using Maxwell's equations the above conditions on $e_\zeta, j_\zeta$ and $J_{0\chi}$ can be rewritten in a more useful form. The $\zeta$ component of equation (2.34) together with equation (2.67) yields :

$$\left.\frac{\partial b_r}{\partial x}\right|_{x=0} = 0 \quad (2.70)$$

From equations (2.65) and (2.66) and the $\zeta$ component of equation (2.32) we obtain :

$$\left.\frac{\partial e_\chi}{\partial x}\right|_{x=0} = 0 \quad (2.71)$$

The $\chi$ component of equation (2.33) enables us to write equation (2.69) in the form :

$$\left.\frac{\partial B_{0\zeta}}{\partial x}\right|_{x=0} = 0 \quad (2.72)$$

At the plasma-vacuum boundary (x=1), the radial component of the oscillating plasma screening current must vanish ; $j_r(1) = j_r(x = 1) = 0$. From equation (2.43) we obtain the equivalent condition that :

$$b_\zeta(1) = 0 \tag{2.73}$$

The steady axial magnetic field must be continuous at the plasma-vacuum boundary and equal to the applied uniform external axial field, $B_{0z}^{ext}$, i.e.

$$B_{0z}|_{x=1} = B_{0z}^{ext}$$

or in terms of helical components, using equation (2.5) :

$$\left.\frac{\kappa x B_{0\chi} + m B_{0\zeta}}{\kappa_0 x}\right|_{x=1} = B_{0z}^{ext} \tag{2.74}$$

The RF magnetic field must also be continuous at the plasma-vacuum boundary. To solve for the magnetic field outside the plasma, we imagine an infinitely thin vacuum layer between the plasma boundary and the helical antenna. The solution of equation (2.15) in this vacuum region is :

$$e_\zeta = \frac{2i\gamma_\omega}{\gamma\kappa_0}(I_1' + cK_1')e^{i(\omega t+\chi)} \tag{2.75}$$

where $c$ is an arbitrary constant. Hence from equation (2.38) we have :

$$b_r = -\frac{2i\gamma_\omega}{\gamma}(I_1' + cK_1')e^{i(\omega t+\chi)} \tag{2.76}$$

$\nabla \cdot \mathbf{b} = 0$ can be used to determine the $\chi$ component of the vacuum RF magnetic field :

$$b_\chi = \frac{i}{\kappa_0 x}\frac{\partial}{\partial x}(x b_r) \tag{2.77}$$

which yields the result :

$$b_\chi = \frac{2\gamma_\omega}{\gamma\kappa_0 x}\left[I_1' + cK_1' + \kappa x(I_1'' + cK_1'')\right] e^{i(\omega t+\chi)} \tag{2.78}$$

The requirement that the RF magnetic field must be continuous at the plasma boundary allows the unknown constant $c$ to be eliminated from equations (2.76) and (2.78). We arrive at the boundary condition :

$$[i\mathrm{b}_r(\mathrm{K}_1' + \kappa \mathrm{x}\mathrm{K}_1'') - \kappa_0 \mathrm{x}\mathrm{b}_\chi \mathrm{K}_1']_{\mathrm{X}=1} = \frac{2\gamma_\omega \kappa_0^2(1)}{\gamma \kappa^2} e^{i(\omega t + \chi)} \qquad (2.79)$$

where $\kappa_0^2(1) = \kappa_0^2(\mathrm{x} = 1)$ and the righthandside has been considerably simplified with the use of Bessel function relations. Equation (2.79) allows us to determine the vacuum magnetic field (via $\gamma_\omega$) necessary to produce the desired RF magnetic field inside the plasma for the chosen values of the external fields and plasma parameters. The degree of penetration of the RF magnetic field into the plasma is thus determined.

## 2.6 Solution of the Current Drive Equations

### 2.6.1 Analytic Solutions

There are two important limits in which the equations presented in Section 2.4 can be solved analytically. These limits are specified in terms of the dimensionless parameters $\gamma$ and $\lambda$ introduced earlier.

In the first limit ($\gamma, \lambda \rightarrow 0$), the effect of the Hall term in Ohm's law is neglected. This limit applies to the case of very small RF field amplitudes, $B_\omega$, or very resistive plasmas ($\eta \rightarrow \infty$) and yields a solution which corresponds to the classical skin effect. The applied RF field is prevented from penetrating into the interior of the plasma by large induced screening currents and is confined to a thin layer at the surface of the plasma with thickness equal to the classical skin depth $\delta$. This limit is not considered to be very interesting in the context of non-linear Hall-effect current drive and will not be treated in any detail here.

In the second, strongly non-linear limit ($\gamma/\lambda^2 \gg 1$, with $\gamma, \lambda$ both large), the Hall term dominates the resistive term in Ohm's law. This limit describes cases where the applied RF field amplitude is large ($B_\omega \gg \mu_0 n e \omega a^2$) and the plasma resistivity

is small ($\eta \rightarrow 0$). In this limit we find that the oscillating plasma screening currents vanish and the RF magnetic field completely penetrates the plasma ($\gamma = \gamma_\omega$), so that its amplitude is everywhere equal to that in the presence of a vacuum. Under these conditions of full penetration, the electron fluid moves in synchronism with the applied RF field resulting in large steady plasma currents being driven. Analytic expressions for the fields and currents inside the plasma in the above limit are derived below. From equation (2.57), in the limit $\gamma/\lambda^2 \gg 1$ we have :

$$\mathrm{b}_\zeta = 0 \tag{2.80}$$

and hence from equation (2.43) :

$$\mathrm{j}_r = 0 \tag{2.81}$$

Equations (2.60) and (2.61) yield for the $\chi$ and $\zeta$ components of the steady driven plasma current, $\mathrm{J}_{0\chi}$ and $\mathrm{J}_{0\zeta}$ respectively :

$$\mathrm{J}_{0\chi} = \frac{1}{\kappa_0} \tag{2.82}$$

$$\mathrm{J}_{0\zeta} = \frac{1}{|\mathrm{b}_r|^2}\mathrm{Re}\{\mathrm{e}_\chi \mathrm{b}_r^*\} \tag{2.83}$$

Substituting the above expression for $\mathrm{J}_{0\chi}$ into equation (2.64) we find :

$$\mathrm{j}_\zeta = 0 \tag{2.84}$$

Equations (2.55) and (2.56) are now closed and can be solved for the $r$ and $\chi$ components of the RF magnetic field :

$$\frac{\partial}{\partial \mathrm{x}}(\mathrm{x}\mathrm{b}_r) = -i\kappa_0 \mathrm{x}\mathrm{b}_\chi$$

$$\frac{\partial}{\partial \mathrm{x}}\left(\frac{\mathrm{b}_\chi}{\kappa_0}\right) = i\mathrm{b}_r$$

The solution of these equations which matches the external RF field at the plasma boundary ($\mathrm{x} = 1$) and also satisfies the requirement of being finite valued at the origin is :

$$\mathrm{b}_r = \frac{-2i\gamma_\omega}{\gamma}\mathrm{I}_1'(\kappa \mathrm{x}) \tag{2.85}$$

$$\mathrm{b}_\chi = \frac{2\kappa_0\gamma_\omega}{\gamma\kappa}\mathrm{I}_1(\kappa \mathrm{x}) \tag{2.86}$$

where the external field is assumed to be $m = 1$. The RF magnetic field in the plasma, whose components are given by equations (2.80),(2.85) and (2.86), is the same as the vacuum magnetic field calculated in Section 2.3 . The externally applied RF magnetic field is said to be fully penetrated.

Taking the real part of equation (2.54) we find that since the righthand side is purely imaginary :

$$\mathrm{Re}\{e_\chi\} = 0 \tag{2.87}$$

From equations (2.63) and (2.83) it then follows that :

$$j_\chi = 0 \tag{2.88}$$

From equations (2.62) and (2.83) we have :

$$\begin{aligned} e_r &= -J_{0\zeta} b_\chi \\ &= -\frac{b_\chi}{|b_r|^2}\mathrm{Re}\{e_\chi b_r^*\} \end{aligned} \tag{2.89}$$

Substituting the above expression for $e_r$ into equation (2.54) and using the solution for the RF magnetic field given in equations (2.80),(2.85) and (2.86), we obtain the following equation for $\mathrm{Im}\{e_\chi\}$ :

$$\frac{\partial}{\partial x}\left(\frac{\mathrm{Im}\{e_\chi\}}{\kappa_0}\right) = \frac{\kappa_0 I_1}{\kappa I_1'}\mathrm{Im}\{e_\chi\} + \frac{\gamma_\omega}{\gamma}\frac{4\kappa}{\kappa_0^4 x^2} I_1'(\kappa x) \tag{2.90}$$

which, incorporating equation (2.87), has the solution :

$$e_\chi = \frac{-2i\gamma_\omega}{\gamma}\frac{\kappa(1-2x^2)}{(2+\kappa^2)\kappa_0 x} I_1'(\kappa x) \tag{2.91}$$

Hence from equations (2.83) and (2.85) we find :

$$J_{0\zeta} = \frac{\kappa(1-2x^2)}{(2+\kappa^2)\kappa_0 x} \tag{2.92}$$

Equations (2.58) and (2.59) when solved for the steady magnetic field $\mathbf{B}_0$ yield :

$$B_{0\zeta} = \frac{1}{\kappa_0 x}\left[-\frac{x^2}{2} + \frac{1}{2+\kappa^2} + B_{0z}^{ext}\right] \tag{2.93}$$

$$B_{0\chi} = \frac{\kappa}{\kappa_0}\left[\frac{3-2x^2}{2(2+\kappa^2)} + B_{0z}^{ext}\right] \tag{2.94}$$

where $B_{0z}^{ext}$ is the steady uniform external axial magnetic field (normalised to $\mu_0 ne\omega a^2$).

The expressions for the steady driven current density and steady magnetic field, $\mathbf{J}_0$ and $\mathbf{B}_0$, are simpler when given in terms of their cylindrical components. Using the co-ordinate transformation equations (2.4),(2.5) and the expressions for $J_{0x}, J_{0\zeta}, B_{0x}, B_{0\zeta}$ just derived, we obtain the results :

$$J_{0\theta} = \frac{2x}{2+\kappa^2} \tag{2.95}$$

$$J_{0z} = \frac{\kappa}{2+\kappa^2} \tag{2.96}$$

$$B_{0\theta} = \frac{\kappa x}{2(2+\kappa^2)} \tag{2.97}$$

$$B_{0z} = B_{0z}^{ext} + \frac{1-x^2}{2+\kappa^2} \tag{2.98}$$

Equations (2.95) and (2.96) are the same as those obtained by BERTRAM(1987) and show that the azimuthal current density increases linearly with radius whilst the axial current density is uniform. Radial profiles of the current density for several values of the parameter $\kappa$ are shown in Figure 2.3.

The $\theta$ and $z$ components of the current density can be integrated to give the steady driven azimuthal (poloidal) current per unit length and the steady axial (toroidal) current respectively :

$$\frac{I_{0\theta}}{ne\omega a^2} = \int_0^1 dx\, J_{0\theta}(x) = \frac{1}{2+\kappa^2} \tag{2.99}$$

$$\frac{I_{0z}}{ne\omega a\pi a^2} = \frac{\kappa}{2+\kappa^2} \tag{2.100}$$

Equations (2.99) and (2.100) represent the maximum possible currents which can be driven for a given value of $\kappa$ (inverse pitch length of the external coil structure). Figure 2.4 shows the dependence of the magnitude of the steady driven currents on the parameter $\kappa = 2\pi a/\ell$ for the case of full penetration. Maximum axial (toroidal) current drive is achieved with $\kappa = \sqrt{2}$, rather than $\kappa \simeq 1.35$ as previously stated by DUTCH,MCCARTHY AND STORER(1986).

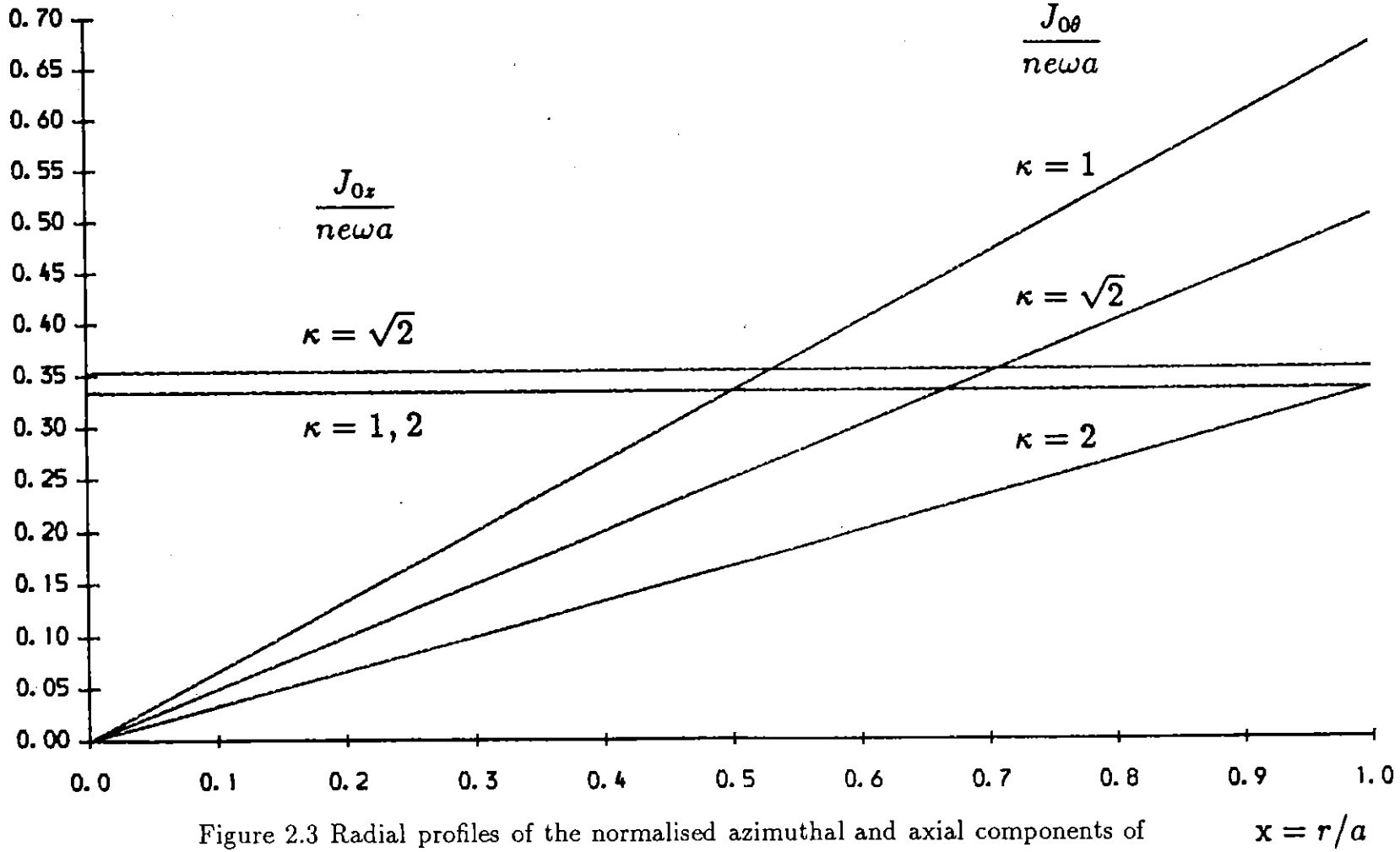


Figure 2.3 Radial profiles of the normalised azimuthal and axial components of the steady driven current density for three values of the parameter $\kappa$. The current densities are for the case of full penetration (strongly non-linear limit) calculated using equations (2.95) and (2.96).

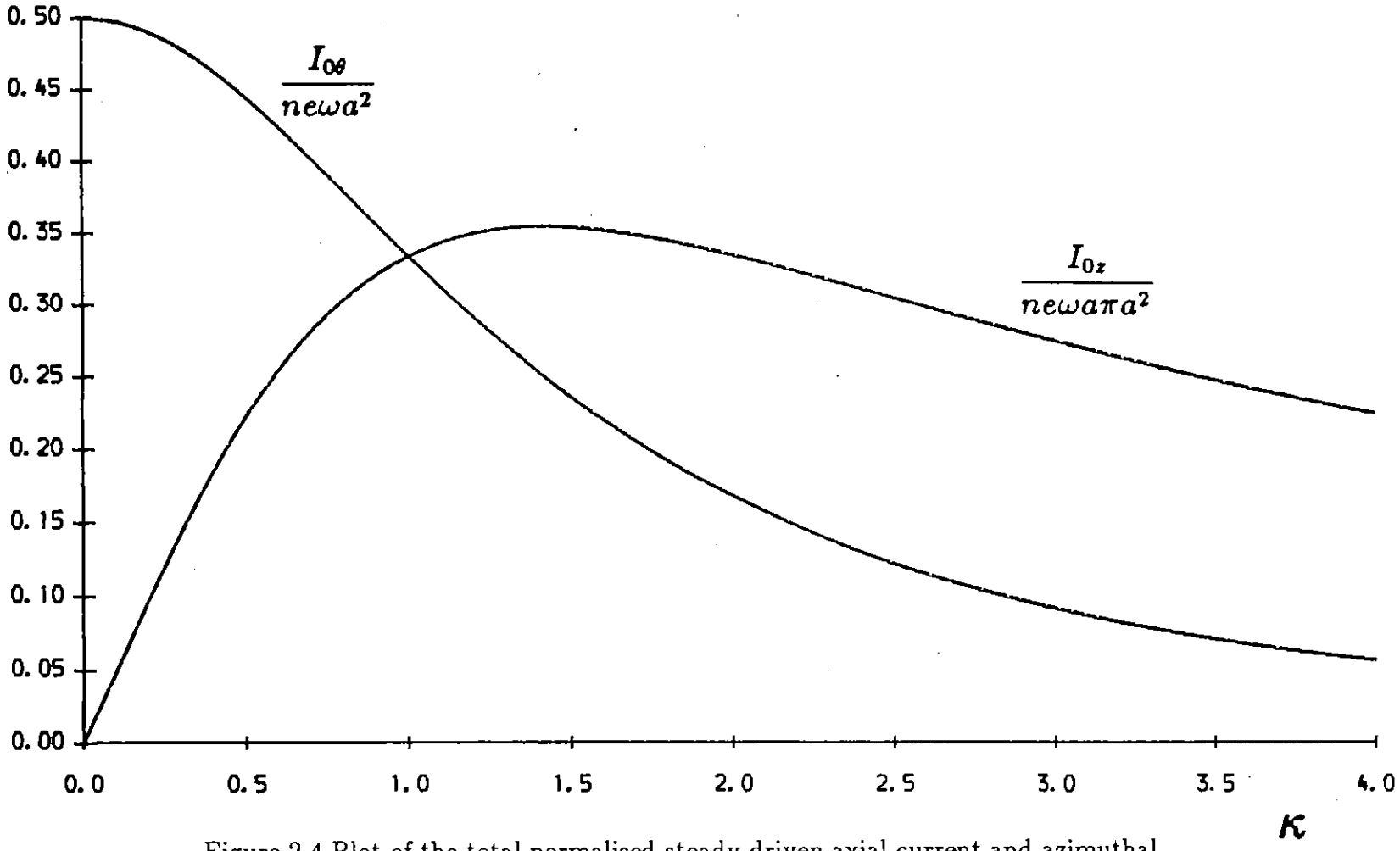


Figure 2.4 Plot of the total normalised steady driven axial current and azimuthal current per unit length versus $\kappa$ for the case of full penetration given in equations (2.100) and (2.99). Maximum axial current is driven when $\kappa = \sqrt{2}$.

### 2.6.2 Numerical Solution

For intermediate values of the plasma parameters $(\gamma, \lambda)$ the current drive equations together with the appropriate boundary conditions are solved numerically. The set of coupled differential equations were numerically integrated from x = 0 to x = 1 using a multiple shooting technique.

From equations (2.70),(2.71) and (2.72) it is clear that $b_r(0), e_\chi(0)$ and $B_{0\zeta}(0)$ are as yet undetermined. The unknown $b_r(0)$ was eliminated by solving for the fields normalised to $b_r(0)$, as mentioned in Section 2.4. The remaining unknowns $e_\chi(0)$ [actually $j_\chi(0)$] and $B_{0\zeta}(0)$ were used as shooting parameters whose correct values were determined from the requirement that the solution satisfied the boundary conditions at x = 1.

The boundary condition on the RF magnetic field at x = 1, equation (2.79), enables the external vacuum magnetic field strength, $B_\omega$, to be determined. The value of $B_\omega$ obtained in this manner can be used to renormalise the fields in the plasma to those in vacuo.

The set of complex coupled differential equations and complex algebraic equations derived in Section 2.4 were solved as a set of ten real first-order coupled differential equations and eight real algebraic equations in the real variables $Y_1 \rightarrow Y_{18}$ where :

$$
\begin{aligned}
x b_r &= Y_1 + iY_2 \\
\frac{b_\chi}{\kappa_0} &= Y_3 + iY_4 \\
\kappa_0 x b_\zeta &= Y_5 + iY_6 \\
\frac{e_\chi}{\kappa_0} &= Y_7 + iY_8 \\
\frac{B_{0\chi}}{\kappa_0} &= Y_9 \\
\kappa_0 x B_{0\zeta} &= Y_{10} \\
J_{0\chi} &= Y_{11} \\
J_{0\zeta} &= Y_{12}
\end{aligned}
$$

$$
\begin{aligned}
\mathrm{j}_{\mathrm{x}} &= Y_{13} + iY_{14} \\
\mathrm{j}_{\zeta} &= Y_{15} + iY_{16} \\
\mathrm{e}_{r} &= Y_{17} + iY_{18}
\end{aligned}
$$

The derivatives are denoted by :

$$
Y_i' = \frac{\partial Y_i}{\partial \mathrm{x}} \qquad i = 1, \cdots, 10
$$

The normalised equations written in terms of the real $Y$ variables are :

$$
\begin{aligned}
Y_1' &= \kappa_0^2 \mathrm{x} Y_4 && (2.101)\\
Y_2' &= -\kappa_0^2 \mathrm{x} Y_3 && (2.102)\\
Y_3' &= \frac{2\lambda^2}{\gamma\kappa_0} Y_{15} - \frac{1}{\mathrm{x}} Y_2 + \frac{2\kappa}{\kappa_0^4 \mathrm{x}^3} Y_5 && (2.103)\\
Y_4' &= \frac{2\lambda^2}{\gamma\kappa_0} Y_{16} + \frac{1}{\mathrm{x}} Y_1 + \frac{2\kappa}{\kappa_0^4 \mathrm{x}^3} Y_6 && (2.104)\\
Y_5' &= -\frac{2\lambda^2}{\gamma} \kappa_0 \mathrm{x} Y_{13} && (2.105)\\
Y_6' &= -\frac{2\lambda^2}{\gamma} \kappa_0 \mathrm{x} Y_{14} && (2.106)\\
Y_7' &= -Y_{18} + \frac{1}{\kappa_0^2 \mathrm{x}} Y_6 - \frac{2\kappa}{\kappa_0^4 \mathrm{x}^3} Y_1 && (2.107)\\
Y_8' &= Y_{17} - \frac{1}{\kappa_0^2 \mathrm{x}} Y_5 - \frac{2\kappa}{\kappa_0^4 \mathrm{x}^3} Y_2 && (2.108)\\
Y_9' &= \frac{2\lambda^2}{\gamma\kappa_0} Y_{12} + \frac{2\kappa}{\kappa_0^4 \mathrm{x}^3} Y_{10} && (2.109)\\
Y_{10}' &= -\frac{2\lambda^2}{\gamma} \kappa_0 \mathrm{x} Y_{11} && (2.110)
\end{aligned}
$$

$$
Y_{11} = \left[ \frac{\frac{1}{\kappa_0}(Y_1^2 + Y_2^2) - \frac{\gamma}{2\lambda^2}\kappa_0 Y_9 (Y_1 Y_6 - Y_2 Y_5)}{(Y_1^2 + Y_2^2 + \frac{2\mathrm{X}^2}{\gamma^2})} \right] \qquad (2.111)
$$

$$
Y_{12} = \left[ \frac{\frac{\kappa_0 \mathrm{X}}{2\lambda^2}(Y_3 Y_6 - Y_4 Y_5) + \kappa_0 \mathrm{x}(Y_1 Y_7 + Y_2 Y_8) - \frac{\gamma}{2\lambda^2}\frac{1}{\kappa_0 \mathrm{X}} Y_{10}(Y_1 Y_6 - Y_2 Y_5)}{(Y_1^2 + Y_2^2 + \frac{2\mathrm{X}^2}{\gamma^2})} \right] \qquad (2.112)
$$

$$
Y_{13} = \gamma\kappa_0 Y_7 - \frac{\gamma^2}{2\lambda^2}\frac{1}{\kappa_0 \mathrm{x}^2} Y_6 Y_{10} - \frac{\gamma}{\mathrm{x}} Y_1 Y_{12} \qquad (2.113)
$$

$$Y_{14} = \gamma\kappa_0 Y_8 + \frac{\gamma^2}{2\lambda^2}\frac{1}{\kappa_0 x^2}Y_5 Y_{10} - \frac{\gamma}{x}Y_2 Y_{12} \quad (2.114)$$

$$Y_{15} = -\frac{\gamma}{\kappa_0 x}Y_1 + \frac{\gamma^2}{2\lambda^2}\frac{\kappa_0}{x}Y_6 Y_9 + \frac{\gamma}{x}Y_1 Y_{11} \quad (2.115)$$

$$Y_{16} = -\frac{\gamma}{\kappa_0 x}Y_2 - \frac{\gamma^2}{2\lambda^2}\frac{\kappa_0}{x}Y_5 Y_9 + \frac{\gamma}{x}Y_2 Y_{11} \quad (2.116)$$

$$Y_{17} = \frac{1}{\kappa_0 x}Y_{10} Y_{13} - \kappa_0 Y_9 Y_{15} + \frac{1}{\kappa_0 x}Y_5 Y_{11} - \kappa_0 Y_3 Y_{12} - \frac{1}{2\lambda^2 x}Y_6 \quad (2.117)$$

$$Y_{18} = \frac{1}{\kappa_0 x}Y_{10} Y_{14} - \kappa_0 Y_9 Y_{16} + \frac{1}{\kappa_0 x}Y_6 Y_{11} - \kappa_0 Y_4 Y_{12} + \frac{1}{2\lambda^2 x}Y_5 \quad (2.118)$$

The procedure used to solve the set of equations (2.101)→(2.118) for the fields and currents inside the plasma was as follows. $Y_{10}(0), Y_{13}(0)$ and $Y_{14}(0)$ were used as shooting parameters whose correct values were determined from the requirement that the numerical solution must satisfy the boundary conditions at the edge of the plasma ($x = 1$).

Using the form of equations (2.101)→(2.118) in the limit $x \to 0$ and the boundary conditions at $x = 0$, a self-consistent set of initial values for the variables $Y_1 \to Y_{18}$ at $x = 0$ can be specified in terms of the chosen values of the shooting parameters. Since the equations are singular at $x = 0$, the boundary conditions and initial values are actually specified at some radial position arbitrarily close to the origin ($\delta x \ll 1$). The righthand sides of the differential equations (2.101)→(2.110) can then be calculated and the equations numerically integrated to advance the solution for the variables $Y_1 \to Y_{10}$ to the next radially incremented position. The current values of $Y_1 \to Y_{10}$ are used to calculate revised values for $Y_{11}, Y_{12}$ [using equations (2.111) and (2.112)], which in turn are required to update the values of $Y_{13} \to Y_{16}$ and finally $Y_{17}, Y_{18}$. The righthand sides of equations (2.101)→(2.110) for the current radial position can then be calculated and the above procedure repeated until the solution is advanced to the plasma boundary, $x = 1$. The trial solution obtained using this method is then examined to determine whether the boundary conditions at $x = 1$ are satisfied. If so, the correct solution has been found, otherwise the values of the shooting parameters must be revised and a new trial solution found using the above method.

The Harwell minimization routine VA05AD was used to search for the values of the shooting parameters for which the numerical solutions best satisfied the boundary conditions at x = 1.

In Figures 2.5 → 2.7 we present numerical solutions of the current drive equations which have been calculated for three different pitch lengths of the external RF windings (specified by the value of the parameter $\kappa$). Figures 2.5 → 2.7 each show the variation of the normalised steady driven plasma currents ($I_{0z}/I_{0z}^{max}$ and $I_{0\theta}/I_{0\theta}^{max}$) with $\gamma_\omega$ for three values of $\lambda$. For these calculations there was assumed to be no externally applied steady axial magnetic field. Note the nonlinear dependence of the driven plasma currents on the RF magnetic field strength (via $\gamma_\omega$). Figures 2.5 → 2.7 demonstrate the existence of non-unique solutions to the current drive equations as previously reported by HUGRASS(1985). There is very good agreement between the numerical solutions for the case $\kappa = 0.01$ (Figure 2.5), where the external RF windings are almost straight and parallel, and the corresponding Rotating Magnetic Field (RMF) current drive solutions found by HUGRASS(1985).

Figure 2.8 illustrates the dependence of the normalised steady driven plasma currents on the external axial magnetic field ($B_{0z}^{ext}$) for the case $\kappa = 0.8$ and $\lambda = 4$. Note that the application of a small *diamagnetic* external axial magnetic field increases the magnitude of the driven plasma currents, whilst the presence of a *paramagnetic* external magnetic field is usually detrimental. Figure 2.8 also indicates the existence of an optimum value for the external diamagnetic axial field, which is confirmed by the experiments.

## 2.7 Helical Mesh Vacuum Field.

In this section, we derive an approximate expression for the vacuum magnetic field produced by the helical mesh antenna [DUTCH, MCCARTHY AND STORER (1987)] which is described later in Section 3.6.3 and shown schematically in Figure 3.9c.

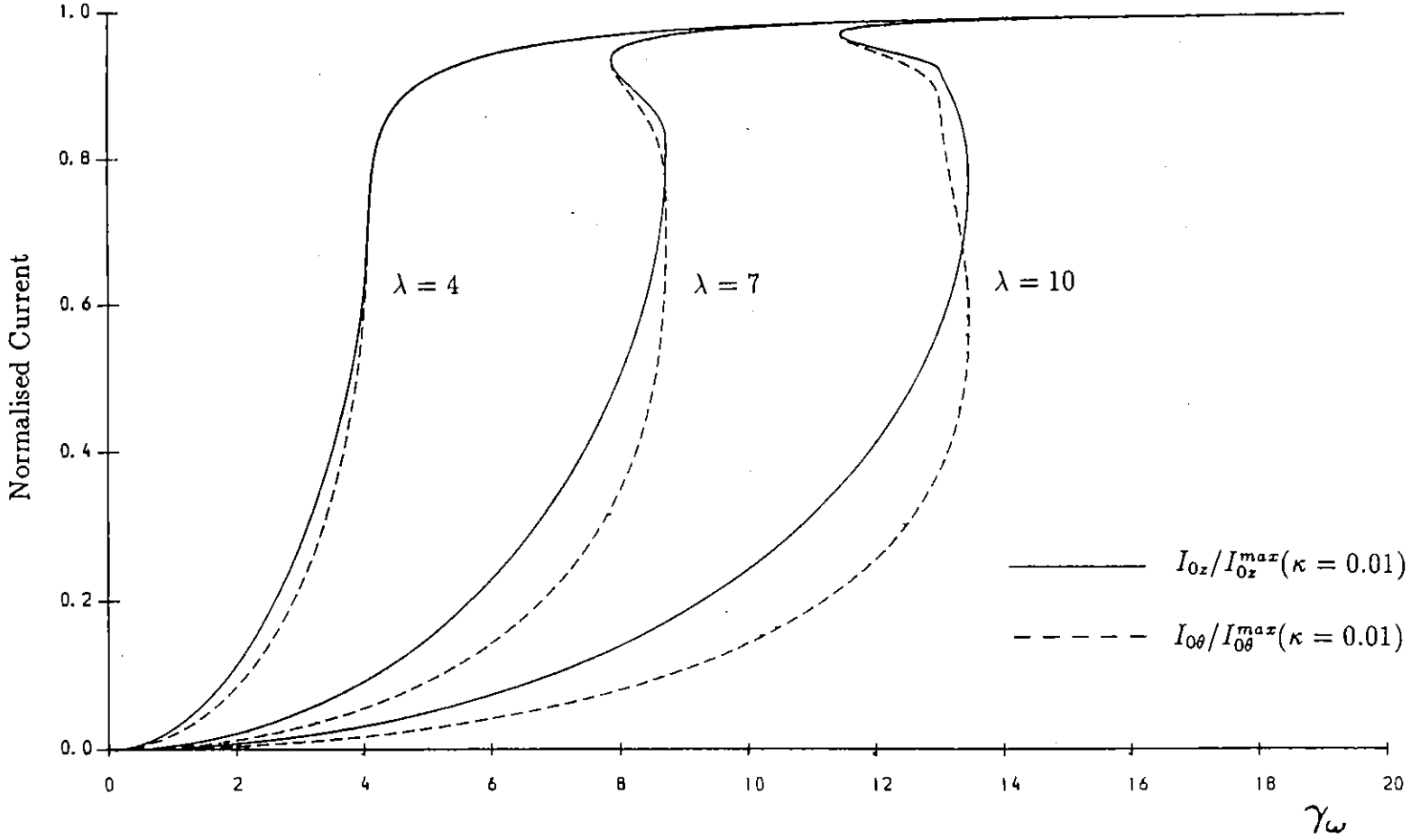


Figure 2.5 The total normalised steady driven axial current ($I_{0z}/I_{0z}^{max}$) and azimuthal current per unit length ($I_{0\theta}/I_{0\theta}^{max}$), for $\kappa = 0.01$. The plasma currents are plotted against the dimensionless parameter $\gamma_\omega$, for three values of the parameter $\lambda$. The curves were obtained by numerical solution of the current drive equations. $I_{0z}^{max}$ and $I_{0\theta}^{max}$ are the maximum steady driven plasma currents for $\kappa = 0.01$, which are calculated from equations (2.99) and (2.100). There is no externally imposed steady axial magnetic field; $B_{0z}^{ext} = 0$.

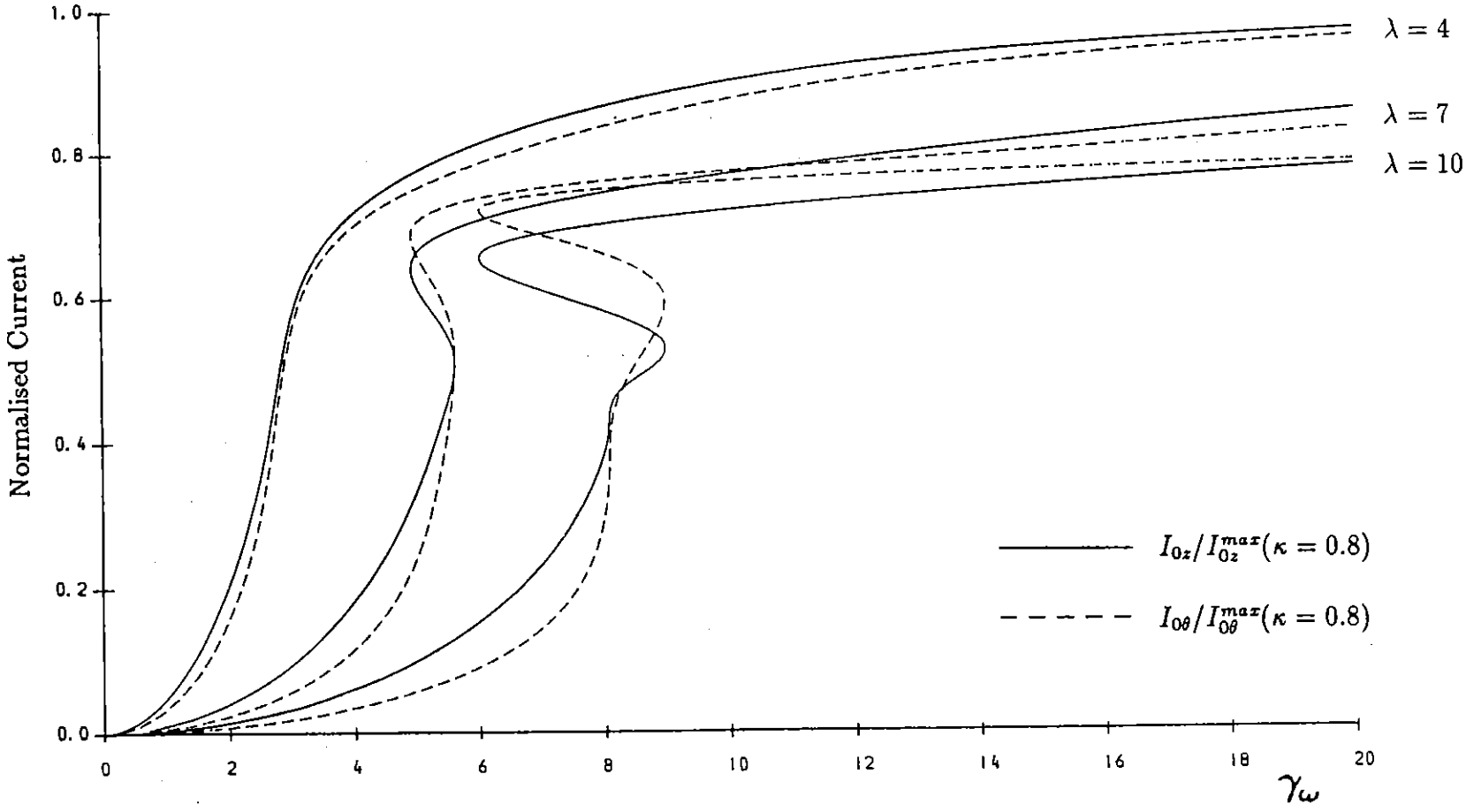


Figure 2.6 Caption reads as for Figure 2.5, except that the inverse pitch length of the external coils is $\kappa = 0.8$ and the steady driven currents are normalised to their maximum values with $\kappa = 0.8$.

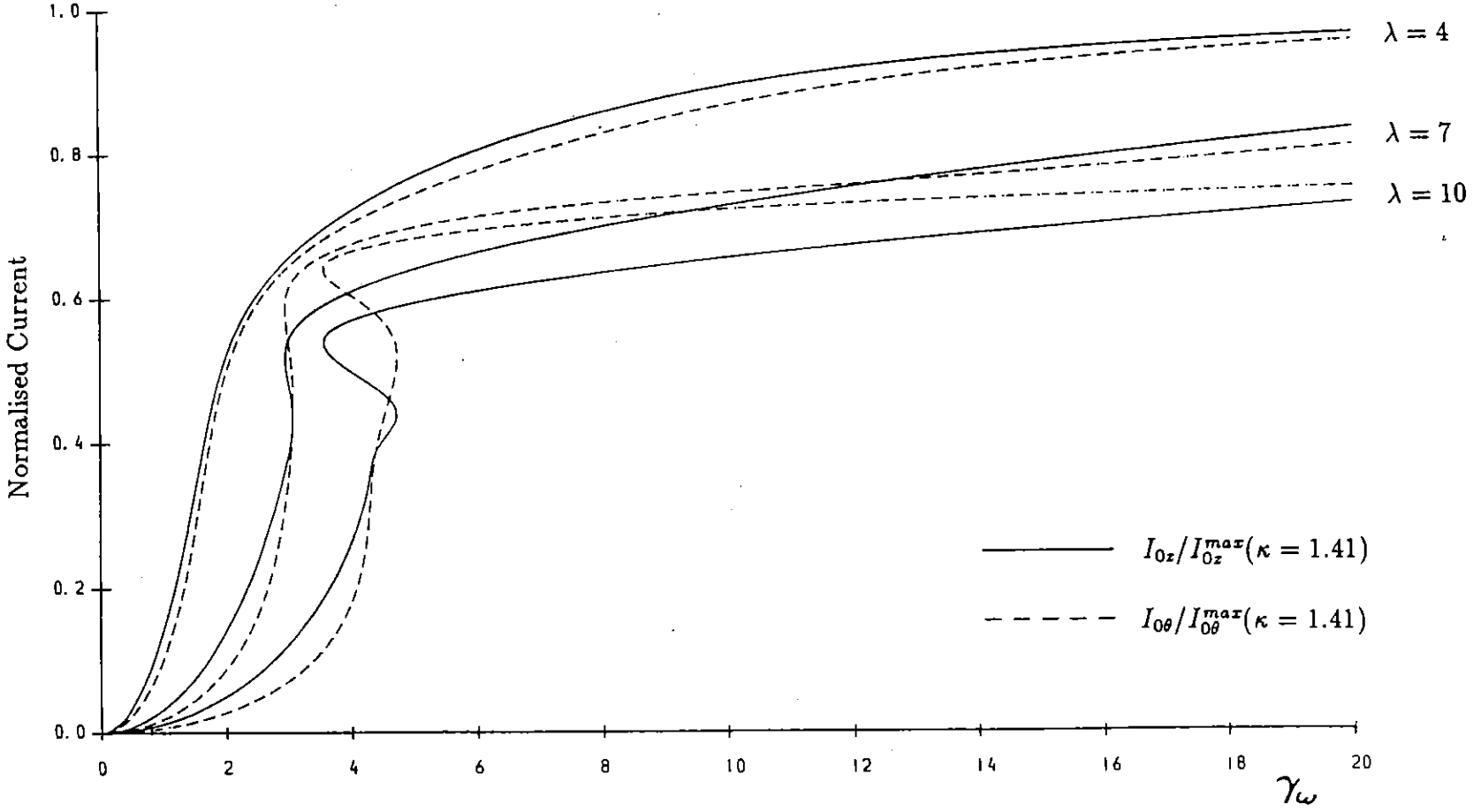


Figure 2.7 The caption again reads as for Figure 2.5, except that $\kappa = 1.41$ and the steady driven currents are normalised to their maximum values with $\kappa = 1.41$.

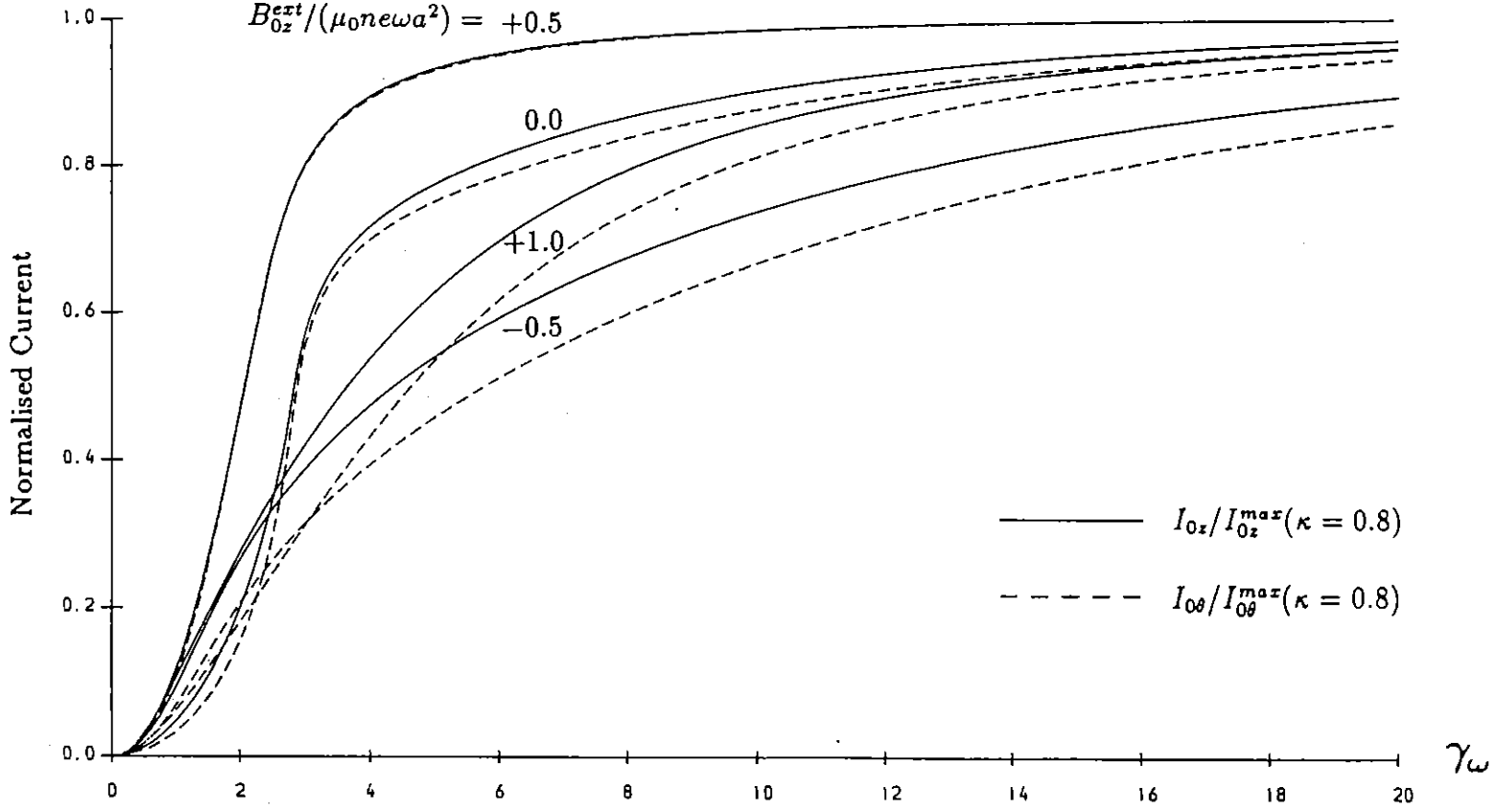


Figure 2.8 Total normalised steady driven axial current ($I_{0z}/I_{0z}^{max}$) and azimuthal current per unit length ($I_{0\theta}/I_{0\theta}^{max}$), for the case $\lambda = 4$ and $\kappa = 0.8$. The driven plasma currents are plotted against the dimensionless parameter $\gamma_\omega$, for four values of the steady normalised externally applied axial magnetic field. A positive value indicates that the applied magnetic field is diamagnetic with respect to the field produced by the driven poloidal current. Similarly, a negative value indicates that the applied magnetic field is paramagnetic. The curves were obtained by numerical solution of the current drive equations. $I_{0z}^{max}$ and $I_{0\theta}^{max}$ are the maximum steady driven plasma currents for $\kappa = 0.8$, which are calculated from equations (2.99) and (2.100).

As the helical mesh antenna consists of a superposed set of $m = +1$ and $m = -1$ double-helix coils, we make use of the vacuum magnetic field calculations for the $m = 1$ double-helix antenna in Section 2.3. The discrete external RF currents are approximated by continuous current distributions and we consider the large aspect ratio cylindrical limit.

In the absence of plasma, the structure fields can be calculated from the individual structure currents and linearly combined. We start from the structure currents represented in the natural helical coordinate systems $(\hat{\boldsymbol{r}}, \hat{\boldsymbol{\chi}}_{+1}, \hat{\boldsymbol{\zeta}}_{+1})$ and $(\hat{\boldsymbol{r}}, \hat{\boldsymbol{\chi}}_{-1}, \hat{\boldsymbol{\zeta}}_{-1})$ for the $m = +1$ and $m = -1$ conductors respectively:

$$\boldsymbol{j}_e = \mathrm{Re}\left[\frac{2I_e}{\pi a} e^{i(\omega t + \chi_{+1})} \hat{\boldsymbol{\zeta}}_{+1} + \frac{2I_e}{\pi a} e^{i(\omega t + \chi_{-1})} \hat{\boldsymbol{\zeta}}_{-1}\right] \delta(r - a) \tag{2.119}$$

which can be written in cylindrical coordinates as:

$$\boldsymbol{j}_e = \mathrm{Re}\left[\frac{2I_e}{\pi a} e^{i(\omega t + \theta + kz)} \left(\frac{-kr\hat{\boldsymbol{\theta}} + \hat{\boldsymbol{z}}}{k_0 r}\right) + \frac{2I_e}{\pi a} e^{i(\omega t - \theta + kz)} \left(\frac{-kr\hat{\boldsymbol{\theta}} - \hat{\boldsymbol{z}}}{k_0 r}\right)\right] \delta(r - a) \tag{2.120}$$

and summed to give:

$$\boldsymbol{j}_e = -\frac{4I_e}{\pi a} \frac{1}{k_0 r} \left[kr \cos(\omega t + kz) \cos(\theta) \hat{\boldsymbol{\theta}} + \sin(\omega t + kz) \sin(\theta) \hat{\boldsymbol{z}}\right] \delta(r - a) \tag{2.121}$$

$I_e$ is the amplitude of the RF currents in the helical conductors which are located at a radius $a$ and have pitch length $\ell = 2\pi/k$, with $k_0 = (k^2 + 1/r^2)^{1/2}$.

The total structure field can be found by using Maxwell's equations in helical coordinates. Using the previous results for the double-helix antenna, equations (2.20) to (2.23), we find:

$$\boldsymbol{b}_e = \mathrm{Re}\left[\begin{array}{l} -2iB_\omega I_1'(kr)\left(e^{i(\omega t + \chi_{+1})} + e^{i(\omega t + \chi_{-1})}\right)\hat{\boldsymbol{r}} \\ +\frac{2B_\omega k_0}{k} I_1(kr)\left(e^{i(\omega t + \chi_{+1})}\hat{\boldsymbol{\chi}}_{+1} + e^{i(\omega t + \chi_{-1})}\hat{\boldsymbol{\chi}}_{-1}\right) \end{array}\right] \tag{2.122}$$

where $B_\omega$ has its usual definition (equation (2.23)) and measures the strength of the RF magnetic field at $r = 0$ for the $m = 1$ double-helix coils. $I_1(kr)$ is a modified Bessel function of order 1.

Expressing the above magnetic field in cylindrical coordinates we get:

$$\boldsymbol{b}_e = \mathrm{Re}\left\{ \begin{array}{l} -2iB_\omega I_1'(kr)\left(e^{i(\omega t+\theta+kz)} + e^{i(\omega t-\theta+kz)}\right)\hat{\boldsymbol{r}} \\ +\frac{2B_\omega k_0}{k} I_1(kr)\left[e^{i(\omega t+\theta+kz)}\left(\frac{\hat{\boldsymbol{\theta}}+k_T\hat{\boldsymbol{z}}}{k_0 T}\right) + e^{i(\omega t-\theta+kz)}\left(\frac{-\hat{\boldsymbol{\theta}}+k_T\hat{\boldsymbol{z}}}{k_0 T}\right)\right] \end{array} \right\} \tag{2.123}$$

i.e.

$$\boldsymbol{b}_e = 4B_\omega \left\{ \begin{array}{l} I_1'(kr)\sin(\omega t + kz)\cos(\theta)\hat{\boldsymbol{r}} \\ -\frac{1}{kr} I_1(kr)\sin(\omega t + kz)\sin(\theta)\hat{\boldsymbol{\theta}} \\ +I_1(kr)\cos(\omega t + kz)\cos(\theta)\hat{\boldsymbol{z}} \end{array} \right\} \tag{2.124}$$

from which we may note immediately that the field has all three spatial components, which progress as a wave on the structure in the axial ($z$) direction as indicated by the $\sin(\omega t + kz)$ dependence, but do not progress in the poloidal direction $\hat{\boldsymbol{\theta}}$.

Immediately we see from the simplest model (of electrons being entrained to move with the field lines provided $eb/m_i \ll \omega \ll eb/m_e$, while ions remain essentially at rest), that net current can be driven in the axial direction but not in the azimuthal (poloidal) direction.

For a more detailed discussion we note that the changing structure fields $\partial \boldsymbol{b}/\partial t$ cause screening currents $\boldsymbol{j}$ to flow in the plasma, which in the case of low resistivity will be out of phase. It is the time averaged cross product of these screening currents with the structure field $\langle \boldsymbol{j} \times \boldsymbol{b} \rangle$ which is identified in the generalised Ohm's law as providing the driving mechanism. Unlike our earlier treatment of this model for double-helix current drive, which is a two-dimensional problem, the analysis of the helical mesh current drive configuration is a three-dimensional problem, whose full analysis must be presented elsewhere.